Neutron-diffraction study of the charge-density wave in α-uranium

J. C. Marmeggi
Laboratoire de Cristallographie, Centre National de la Recherche Scientifique, Boîte Postale 166X, F-38042 Grenoble, France and Universite J. Fourier, F-38000 Grenoble, France

G. H. Lander
Commission of the European Communities, Joint Research Centre, Institute for Transuranium Elements, Postfach 2340, D-7500 Karlsruhe, Federal Republic of Germany

S. van Smaalen
Laboratory of Inorganic Chemistry, Materials Science Center, University of Groningen, NL-9747 AG Groningen, The Netherlands

T. Brückel and C. M. E. Zeyen
Institut Laue Langevin, Boîte Postale 156X, F-38042 Grenoble, France
(Received 29 March 1990)

Neutron-diffraction experiments have been performed on a single crystal of α-U in the phase below 43 K, in which a charge-density wave (CDW) exists. We report on the identification of the superspace group in the CDW state. This is primitive monoclinic, in agreement with recent theoretical predictions. The CDW state below 37 K consists of two coherent **q** vectors existing within the same crystal volume, and this coexistence gives rise to additional interference effects. At 22 K we find that q_y (the component of the CDW in the [010] direction) locks in to a commensurate value of $\frac{1}{6}$. Associated with this lockin, we find higher-order satellites of third, fifth, seventh, and ninth harmonics of the total CDW distortion appearing below 30 K. Elastic diffraction effects extend over six decades of intensity. The presence of higher odd-order harmonics indicates a squaring of the CDW displacement, but this is not complete even at the lowest temperatures. Unusual domain effects are found near the 22-K lock-in phase transition.

I. INTRODUCTION

Uranium is the only nonmagnetic element that has been found to develop a periodic lattice distortion [hereafter referred to as a charge-density wave (CDW)] at low temperature. In fact, *two*, apparently independent, CDW's were discovered almost simultaneously.[1,2] Subsequent experiments characterized the atomic displacements[3] and showed that they were related to the eigenvectors of the phonon mode Σ_4 that softens as a precursor to the CDW phase,[4] which develops at 43 K. A review of the experimental situation up to 1984 is given by Smith and Lander.[5]

We now know that principal CDW in α-U has a **q** vector given by

$$\mathbf{q}=0.500\mathbf{a}^*\pm q_y\mathbf{b}^*\pm q_z\mathbf{c}^* \ , \tag{1}$$

where q_y and q_z were apparently incommensurate at all temperatures and are constant below $\sim$20 K. Previous experiments[2,3] reported $q_y\simeq 0.176$ and $q_z=0.182$ at 10 K. To understand the many modulations occurring in α-U, we present in Fig. 1 a schematic view of a portion of a reciprocal space. As is known from earlier work, the maximum intensity of the CDW satellites is found when the Bragg intensity at the neighboring position is zero. This is essentially because the satellites correspond to the condensation of an optic mode,[5] so whereas the Bragg intensities are proportional to $\cos 2\pi(ky+lz)$, where the U position is $\pm(0y\frac{1}{4})$, the satellite structure factors contain the expression $\sin 2\pi(ky+lz)$. Thus we concentrate our searches around the Bragg point (201), which is forbidden because of the glide plane along the b axis. (The space

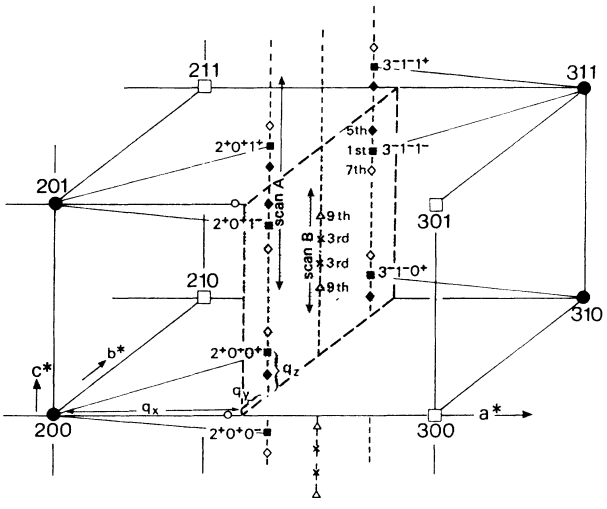

FIG. 1. Schematic of reciprocal space in α-U. Since the high-temperature structure is C face centered, allowed lattice points (solid circles) have $h+k=$even. The non-C-face-centered points are shown as open squares. Satellites are ■ (first), × (third), ♦ (fifth), ◇ (seventh), and △ (ninth). The position of two of the satellites from the secondary modulation—the so-called "Smith" satellites (Ref. 1)—are shown as open circles.

group is *Cmcm* in the high-temperature phase.) Referring to Fig. 1, the maximum satellite intensity is found at $(2^+,0^+,1^+)$, which is a short-hand notation for $(2,0,1)+(q_x,q_y,q_z)$. The distances q_x, q_y, and q_z are marked in Fig. 1. Keeping q_x and q_y fixed, we may proceed along (scan A) the c^* axis (thus performing an l scan) until the next first-order satellite $(2^+,0^+,2^-)$ or $(2^+,0^+,0^+)$ is found. Both of these are weak. In previous experiments,[3] many satellite intensities were measured and the parameters for a (sinusoidal) modulation[3] for the CDW displacement deduced. The most important displacement of the atoms is along the a axis and is about 0.03 Å at low temperature.

The second modulation in α-U gives rise to peaks along the a^* axis but at positions that are commensurate with an apparently *longer* repeat unit cell along the **a** axis.[1,5] The peaks arising from this second modulation are weaker by over an order of magnitude than the peaks from the q vector in Eq. (1), and they also have a different shape. In this paper we will not address this second modulation.

Since the review[5] in 1984, one experimental and two theoretical papers have appeared. Using electron microscopy, Chen and Lander[6] showed that the CDW phase was a multiple-domain state. They also reported on domain growth and reorientation effects that occurred near 22 and 37 K. The theoretical papers by van Smaalen and collaborators[7] focused on the superspace group in the CDW state and the exact nature of the modulation. They proposed the possibility of several multidomain states. Combined with the results of the electron-microscopy study,[6] this led to the suggestion of a superspace group of monoclinic form with a loss of the C-face centering.[7,8] [In the course of determining the modulation, they also noted an error of a factor of 2 in the magnitude of the atomic displacements as given in Refs. 3 and 5. The correct magnitudes with the model of Refs. 3 and 5 are given in Table VI of van Smaalen and George.[7]] We report here on experiments that confirm the loss of the C-face centering and that the superspace group has symmetry lower than orthorhombic. The theoretical paper by Walker[8] treated the phase transitions in terms of a Landau expansion and made certain predictions with respect to the temperature dependence of the wave-vector components at 37 K. Because x-ray work with a synchrotron source has better q resolution than is possible with neutrons [this is particularly true at large Q values, which are necessary because the intensity of the main CDW peaks is approximately proportional to $(\mathbf{Q}\cdot\mathbf{a})^2$], this aspect will be left to a separate publication.[9]

In the course of our studies we have also reexamined the q_y component and found a series of new satellites at low temperature. Their relation to the other satellites is such that a squaring of the modulation develops at low temperature.

II. EXPERIMENTAL DETAILS

The experiments were performed on the D10 diffractometer at the Institut Laue Langevin. A thermal neutron beam passed down a guide tube and was diffracted from a vertically focusing Cu(200) crystal to given a monochromatic beam of 1.26 Å. Because of the guide transmission and use of an analyzer the $\lambda/2$ contamination is very small ($\sim 5\times10^{-5}$ of λ). The instrument has a four-circle arrangement[10] with a cryostat that allows the sample to be cooled to low temperature (1.7 K). The scattered beam may be detected directly or analyzed in a three-axis mode. For most of the symmetry examinations no analyzer was used, but for detecting weak peaks a PG(002) analyzer was useful in reducing background. The crystal of uranium was the largest crystal currently available, a parallelopiped of dimensions $\sim 3\times4\times8$ mm.[3] It was mounted so that the $(h0l)$ plane was in the scattering plane with $X=0$ on the four-circle. Experiments were also performed with the crystal in the $(hk0)$ orientation. For these experiments a beam of 2.36 (or 1.54) Å was used with a pyrolytic graphite filter to reduce $\lambda/2$ and a PG(002) analyzer.

III. EXPERIMENTAL RESULTS

A. Examination of average structure

It is useful to begin this discussion with reference to the intensities observed in α-U, as is illustrated on a logarithmic scale in Fig. 2. We have normalized to the Bragg intensities by reference to earlier work,[3] in which a small crystal was used and absolute intensities obtained. For the (200) intensity the structure factor corresponds to b_U per atom, or $F=1$ in the notation of Refs. 3 and 5. Throughout this paper we will use the same scale for structure factors. Lorentz corrections have been made in every case.

Our first test was of the possible deviation of the atom position, nominally at $\pm(0,y,1/4)$ in the space group *Cmcm*, from the position $z=\frac{1}{4}$. Variations from $z=1/4$ will give rise to reflections $(00l)$ with $l=$odd. A Renninger scan (i.e., a rotation of the crystal about the scattering vector) of the (005) is shown in Fig. 2. Since the C-face centering dictates $h+k=$even, and $(00l)$ reflections satisfy this, enormous multiple scattering effects are expected. Similar scans were already performed by Barrett *et al.*[11] and they states that some "real" scattering was possibly present at the (001) and (003) positions. However, from Fig. 2 we cannot make such a conclusion about the (005). Just because the scans do not drop to the $\lambda/2$ level of $\sim 5\times10^{-5}$ does not mean that "real" scattering is present. We feel that it is more likely that *all* the scattering at (005) is multiple is character. Further experiments, particularly with longer-wavelength neutrons, would be needed to resolve this. Based on the minimum of $\sim 2\times10^{-4}$ in the intensity, we can say that $\epsilon_z \leq 4\times10^{-4}$, where any deviation would result in an atomic z coordinate of $\frac{1}{4}+\epsilon_z$. We have also examined the temperature dependence of the (005) and find *no change* in cooling through 43 K into the CDW state. Thus the change in the z components is $\Delta z \leq 2\times10^{-4}$.

The second test was of the possible loss of the C-face centering in the average structure. Positions such as (100),(300),(341) do not satisfy conditions for strong multiple scattering, because such scattering occurs only at

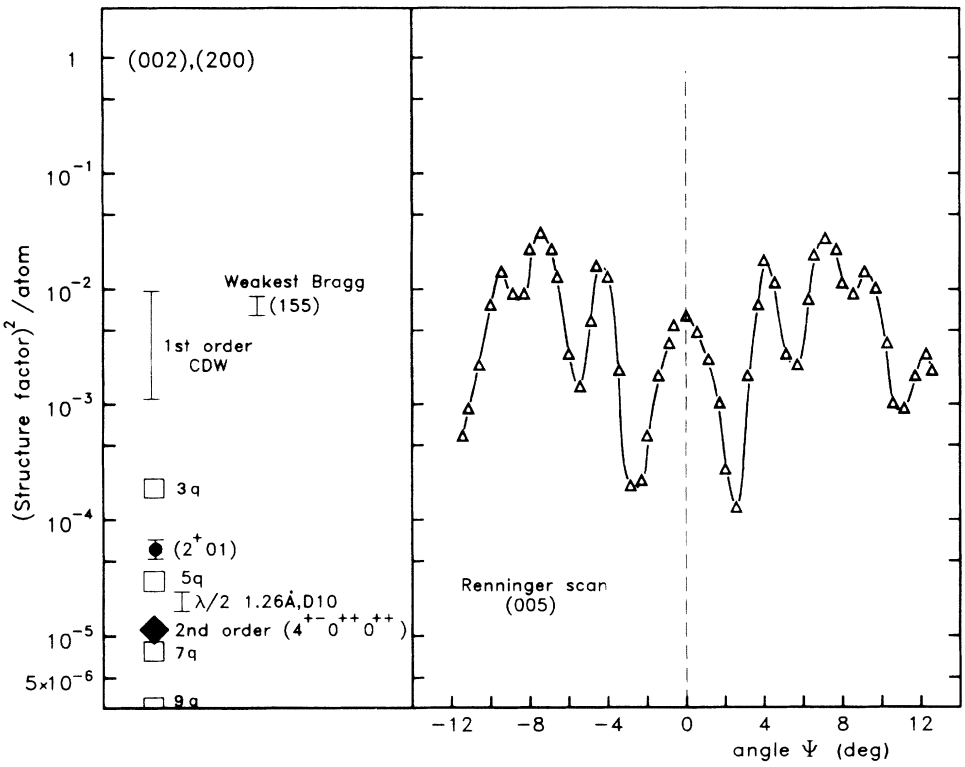

FIG. 2. Schematic of intensities studied for $T \leq 22$ K in α-U on a logarithmatic scale. The strong Bragg reflections are 1 on this scale. Right-hand side: Renninger scan of (005) as a function of the azimuthal angle Ψ around the scattering vector.

$h+k$=even positions. However, they are subject to $\lambda/2$ contamination and multiple scattering involving $\lambda/2$. Since this contamination is so small in our case ($\sim 5\times 10^{-5}$), we can neglect such multiple effects. We have measured a total of 25 reflections, which included 16 independent hkl values, at 60 K and then at 16 K. Average intensities were $\sim 3\times 10^{-5}$ at 60 K, which corresponds to the $\lambda/2$ component (see Fig. 2). On cooling to 16 K there was a definite increase in some, but not all, intensities. For example, all reflections of the form $\{341\}$ increased by $\sim 4\times 10^{-5}$, whereas the $\{342\}$ reflections increased by less than 7×10^{-6}. If the U atom positions are written as $(0,y,\frac{1}{4})$ and $(\epsilon_x, y+\epsilon_y, 1/4)$, one would expect a consistent pattern of intensity changes proportional to h^2, k^2, or $(h+k)^2$. This is not the case. Indeed, we believe ϵ_x and ϵ_y are both $<10^{-4}$.

The increase in intensity of some reflections may be attributed to real second-order satellites in the CDW state. To understand this it is necessary to write down the four possible $\mathbf{q}$ vectors implicit in Eq. (1). Following van Smaalen and George[7] these may be written

$$\begin{aligned}
\mathbf{q}^{(1)} &= (\tfrac{1}{2}, q_y, q_z) , \\
\mathbf{q}^{(2)} &= (\tfrac{1}{2}, -q_y, q_z) , \\
\mathbf{q}^{(3)} &= (\tfrac{1}{2}, q_y, -q_z) , \\
\mathbf{q}^{(4)} &= (\tfrac{1}{2}, -q_y, -q_z) .
\end{aligned} \tag{2}$$

We should note here that confusion may arise over the labeling of $\mathbf{q}^{(i)}$ $(i=1,4)$. We follow here the nomenclature of Ref. 7, but Walker[8] has reversed $\mathbf{q}^{(4)}$ and $\mathbf{q}^{(3)}$. The Walker notation is followed in Ref. 9. Satellites of the form $2\mathbf{q}^{(i)}$, where $\mathbf{q}^{(i)}$ is one of the above sets, were already reported in Ref. 5. However, satellites of the form $\mathbf{q}^{(1)}+\mathbf{q}^{(4)}$ and $\mathbf{q}^{(2)}+\mathbf{q}^{(3)}$ will appear exactly at these $h+k$=odd reflections, as noted in Ref. 7. Reflections of the form $\mathbf{q}^{(1)}-\mathbf{q}^{(4)}$ will appear at new positions in reciprocal space. One of these, at the $(4^{+-}0^{2+}0^{2+})$ position is shown in Fig. 3. The intensity of $\sim 3\times 10^{-5}$ is the same magnitude as the two $\mathbf{q}$ satellites,[5] the biggest of which was found (and calculated) to be $\sim 15\times 10^{-5}$. This is comparable in magnitude to the $\mathbf{q}^{(1)}+\mathbf{q}^{(4)}$ satellite intensity appearing at the (341) position. As the $\mathbf{q}^{(1)}-\mathbf{q}^{(4)}$ are not contaminated with either $\lambda/2$ or possible multiple scattering within the main reciprocal lattice, observation of these reflections (Fig. 3) definitely proves that $\mathbf{q}^{(1)}$ and $\mathbf{q}^{(4)}$ exist within the same domain. This is in agreement with the predictions of van Smaalen and George.[7]

The third test relating to the symmetry was to measure a series of satellite intensities associated with different reflections. These are given in Table I. By measuring satellite intensities around reflections with large h (401), large k (220), and large l (205), we effectively test the presence of the mirror planes m_x, m_y, m_z, respectively, in the average α-U structure in the CDW phase. We find $\sigma I/I \sim 5\%$ for each set of eight reflections. One must

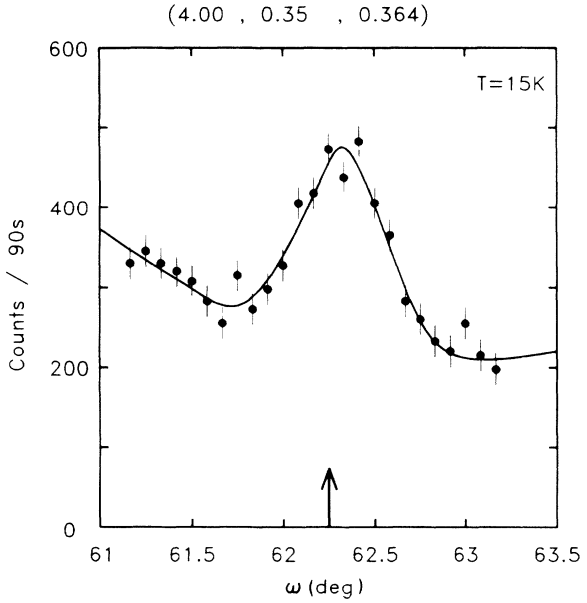

FIG. 3. Scan at $T=15$ K through the position $(4^{+-},0^{2+},0^{2+})$ showing the presence of a second-order satellite of the type $\mathbf{q}^{(1)}-\mathbf{q}^{(4)}$. Because the k resolution is poor in this scan, the value of k is not well defined. Scan performed with $(h0l)$ in scattering plane. The vertical arrow gives the calculated ω value for this reflection.

remember in this process that the intensity will be dependent on the accuracy of q_y and q_z [Eq. (1)], and that path-length differences in the crystal may introduce real variations for which we have made no corrections. From our present data it appears that all mirror planes are present in the average structure. However, these intensities also reflect the domain populations, since all domains are sampled, and some preferential domain population would need to be present to progress further on this point.

B. Examination of the q_x component

In a recent group-theoretical treatment of the CDW, Walker[8] predicted that the q_x component, which at low temperatures has the commensurate value of 1/2, should be incommensurate between 37 and 43 K. To examine this with neutrons is relatively difficult because the CDW peak at 40 K has ~30% of its intensity at 10 K, and the peaks start to broaden. We have made a series of contour scans to determine the center of gravity of the satellite peaks at 40 K and find that $q_x=0.495(3)$. Thus, the neutron experiments do suggest that Walker's prediction is correct and q_x becomes incommensurate.

In a separate paper,[9] this question of the q_x wave vector is addressed by using the much higher resolution and intensity available with an x-ray synchrotron source.

C. Examination of the q_y component

Early experiments[2,5] gave the value of q_y as 0.176(2) at 10 K, decreasing to ~0.12 near 40 K. We have reexamined the variation of q_y with the crystal mounted with $(hk0)$ in the scattering plane to give the highest precision in determining q_y, and the results are shown in Fig. 4. From this figure it is clear that the 22-K transition, which was first identified by thermal-expansion measurements by Steinitz *et al.*,[12] is the temperature at which q_y locks in to a commensurate value of 1/6. The discontinuity in q_y we find near 22 K is in good agreement with the claim that the transition is first order.[12] This temperature of 22 K is also the one at which the electron microscopy studies[6] first see domain motion.

D. Observation of higher harmonics

The 2q satellites were already observed by Smith and Lander,[5] and have essentially the intensity expected for a sinusoidal displacement wave. With this model the 3q satellites and higher orders should be unobservable. The second-order satellites of the form $(4^{2-}0^{2+}2^{2+})$ are shown in Fig. 7 of Ref. 5 and are $\sim 10^{-5}$ on the intensity scale of Fig. 2 of this paper. For the third-order satellites as calculated with a simple sinusoidal displacement model the intensities are down to $<10^{-6}$ and too small for us to observe. However, when a commensurate modulation of the CDW occurs, a gain in energy is achieved if the modulation is squared, i.e., over long regions of the crystal the displacements on all atoms are similar. As is well known, a squaring of the modulation involves the development of *odd* harmonics in the q modulation leading to odd-order satellites in the diffraction pattern, $n=1$, 3, 5, 7, 9, etc.

The lock-in transition $q_y=1/6$ (and as we shall see below the probable commensurate value of q_z) at 22 K apparently causes higher-order satellites to appear. We first discovered these (essentially by accident) by scanning along the l direction, but with q_x and q_y set corresponding to the first-order CDW values. A representative scan is shown in Fig. 5. This is scan A in Fig. 1. From this

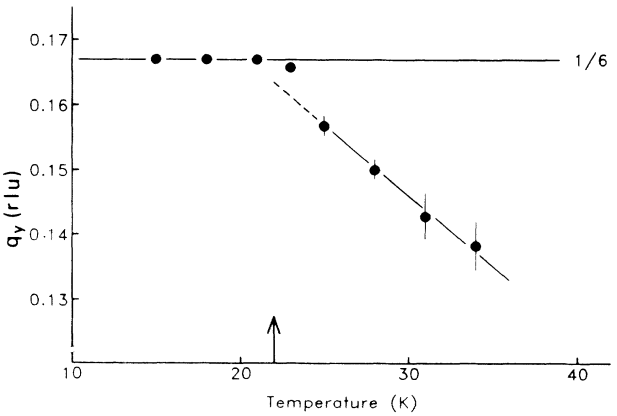

FIG. 4. Variation of the q_y component (in reciprocal-lattice units), performed with $(hk0)$ in scattering plane, as a function of increasing temperature and using the first-order satellites. The vertical arrow marks 22 K, at which thermal expansion work (Ref. 12) indicated a first-order transition.

scan and a number of others the following qualitative statements may be made.

(1) The peaks are symmetric about the position l=integer. The satellite close to the integer value of l has an integrated intensity of ~2% of the nearest first-order satellite and this ratio is approximately constant for the six reciprocal-lattice points examined. For example, at $(2^+,0^+,2^\pm)$ the first-order satellites are very weak and we cannot observe the extra satellites.

(2) The weaker satellites are ~0.5% of the closest first-order satellite intensity.

(3) Both satellites are exactly parallel to **c*** and have

TABLE I. Intensities testing mirror planes m_x, m_y, and m_z in the satellite intensities of α-U. The average intensities are followed by the standard deviation derived from the measured set. All intensities are in units of 10^{-5}, see Fig. 2.

h	k	l	satellite			I	Average I	Calculated I
4	0	1	−	+	+	929±10		
			−	−	+	827		
		−1	−	+	−	876		
			−	−	−	901		
−4	0	1	+	+	+	953		
			+	−	+	843		
		−1	+	+	−	855		
			+	−	−	829	877±44	902.5
4	0	1	−	+	−	978±12		
			−	−	−	961		
		−1	−	+	+	1072		
			−	−	+	927		
−4	0	1	+	+	−	947		
			+	−	−	943		
		−1	+	+	+	1050		
			+	−	+	937	977±51	960.4
2	2	0	−	+	+	182±5		
			−	+	−	173		
2	−2	0	−	−	+	178		
			−	−	−	189		
−2	2	0	+	+	+	180		
			+	+	−	180		
−2	−2	0	+	−	+	178		
			+	−	−	182	180±5	173.8
2	2	0	−	−	+	134±5		
			−	−	−	177		
2	−2	0	−	+	+	193		
			−	+	−	164		
−2	2	0	+	−	+	153		
			+	−	−	168		
−2	−2	0	+	+	+	181		
			+	+	−	149	165±17	178.1
2	0	5	−	+	+	131±4		
			−	−	+	122		
		−5	−	+	−	135		
			−	−	−	122		
−2	0	5	+	+	+	125		
			+	−	+	121		
		−5	+	+	−	130		
			+	−	−	125	126±5	126.7
2	0	5	−	+	−	291±8		
			−	−	−	308		
		−5	−	+	+	330		
			−	−	+	282		
−2	0	5	+	+	−	292		
			+	−	−	303		
		−5	+	+	+	320		
			+	−	+	283	300±16	285.1

values of q_x and q_y identical to those of the first-order satellites.

(4) Both satellites are considerably broadened in the q_z direction; they are at least a factor of 3 wider than the resolution function. Thus their peak intensities are less than 1% of the main CDW peak, and the weak peak has an intensity of $\sim 2\times 10^{-5}$ of the Bragg peak (see Fig. 2).

The indexing of Fig. 5 is based on the l coordinate only and determines a q_z component of 0.1846(12) rlu (reciprocal-lattice unit). However, these satellites are 5**q** and 7**q** harmonics of the *total* CDW modulation. This may be seen by recalling that

$$5\mathbf{q}=5(\tfrac{1}{2},1/6,q_z)=(n+\tfrac{1}{2},m-1/6,5q_z)\ ,$$

$$7\mathbf{q}=7(\tfrac{1}{2},1/6,q_z)=(n+\tfrac{1}{2},m+1/6,7q_z)\ ,$$

where n and m are integers. Actually, indexing these peaks is more complex and we must find the reciprocal-lattice point related by these higher-order harmonics. Thus, in order of increasing l across Fig. 5 we have

$$2^{-7}\text{: } (-1,-1,2)-7(-\mathbf{q}^{(3)})\ ,$$

$$1^{-1}\text{: } (2,0,1)-1(-\mathbf{q}^{(3)})\ ,$$

$$0^{+5}\text{: } (5,1,0)+5(-\mathbf{q}^{(3)})\ ,$$

$$2^{-5}\text{: } (5,1,2)-5\mathbf{q}^{(1)}\ ,$$

$$1^{+1}\text{: } (2,0,1)+\mathbf{q}^{(1)}\ ,$$

$$0^{+7}\text{: } (-1,-1,0)+7\mathbf{q}^{(1)}\ .$$

An alternative indexing involving $\mathbf{q}^{(1)}$ and $\mathbf{q}^{(3)}$ requires starting from a reciprocal-lattice point that has $h+k=$odd. By choosing the line $(2.5,-0.167,l)$ we would sample q vectors $\mathbf{q}^{(2)}$ and $\mathbf{q}^{(4)}$. Our measurements show, as expected, that the volume of the various domains within the crystal are equivalent.

We have used Gaussian curves to fit the scans in Fig. 5. The first-order peaks are essentially resolution limited (i.e., the same width as nuclear Bragg peaks made with a comparable scan) in the neutron case. However, to fit the base of the first-order peaks we need to introduce a second Gaussian at the same value of l but with a peak intensity $\sim 6\%$ of the main first-order peak and significantly greater width, full width at half maximum (FWHM) ~ 0.05 rlu, as opposed to the 0.018 rlu of the resolution function. The physical origin of these extra contributions to the first-order peaks is unclear, but we have determined that it is probably instrumental, or connected with the crystal, as it can be observed also for the Bragg peaks. We should emphasize that this contribution is only evident when the intensities are plotted on a logarithmic scale and does not affect the determination of a (FWHM) as the second Gaussian is at the $\sim 6\%$ level compared to the strong main component.

Third-order satellites will lie along a line in reciprocal space denoted by $q_y=\frac{1}{2}=3q_y$ below 22 K. Similarly, ninth-order satellites are found at a position given by (integer$\pm 3q_y$). A scan of such satellites is shown in Fig. 6. Reference should be make to "scan *B*" of Fig. 1 to see where these satellites occur in reciprocal space. Since $3q_y=\frac{1}{2}$ for $T<22$ K, the third (and ninth) -order satellites may be indexed by considering (integer$\pm 3q_y$). Thus in order of increasing l across Fig. 6 we have

$$2^{-9}\text{: } (-2,2,2)-9(-\mathbf{q}^{(4)}) \text{ and } (7,-1,2)-9(\mathbf{q}^{(2)})\ ,$$

$$1^{-3}\text{: } (1,1,1)-3(-\mathbf{q}^{(4)}) \text{ and } (4,0,1)-3(\mathbf{q}^{(2)})\ ,$$

$$0^{+3}\text{: } (1,1,0)+3(\mathbf{q}^{(2)}) \text{ and } (4,0,0)+3(-\mathbf{q}^{(4)})\ ,$$

$$-1^{+9}\text{: } (-2,2,-1)+9(\mathbf{q}^{(2)}) \text{ and } (7,-1,-1)+9(-\mathbf{q}^{(4)})\ ,$$

where the indexing using $\mathbf{q}^{(2)}$ and $\mathbf{q}^{(4)}$ indicate that the sa-

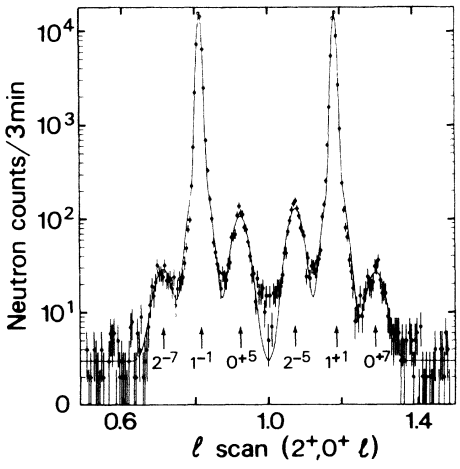

FIG. 5. Scan at 15 K along the line (2.5,0.167,l) with l varying from 0.6 to 1.4. The indexing of the diffraction maxima is given as $L+nq_z$, with integer L and n indicated as L^n. The lines are fits to the data points with Gaussian functions as explained in the text (scan *A* in Fig. 1).

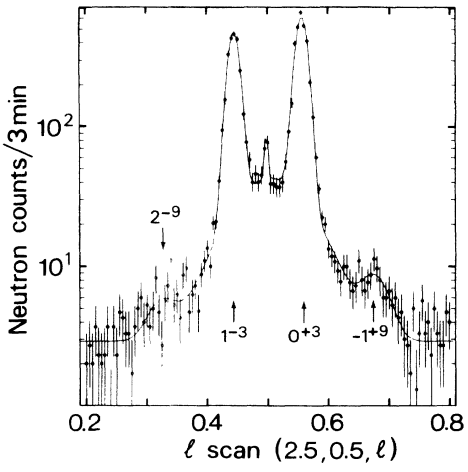

FIG. 6. Scan at 15 K along the line (2.5,0.5l) in reciprocal space (scan *B* in Fig. 1). The lines are fits to the data points with Gaussian functions. The small sharp peaks at (2.5,0.5,0.5) is the $\lambda/2$ component from the (511) reflection. The ninth-order peak at $l\sim 0.34$ is not clearly visible with our present statistics but an appropriate Gaussian has been drawn to indicate the position. The count scale is same as Fig. 5, although in practice 9 min/pt was used.

tellites come from different domains. However, because at low temperature $q_y=\frac{1}{6}$ and $q_x=\frac{1}{2}$, in each case the two rays coincide *at the same* place for $T<22$ K. These do not involve the same volume of the crystal so the intensities rather than amplitudes are added. At higher temperatures when $q_y\neq\frac{1}{6}$ it is in principle possible to separate these peaks, but our k resolution in the $(h0l)$ orientation, in which Fig. 6 was taken, is poor ($\sim$0.034 rlu) so that this is by no means easy. We have found that in the few cases considered the intensities of the two rays are not equal, with one being 3 or 4 times as strong as the other. A further separation is not possible at this stage.

We have seen previously that the positions of the fifth- and seventh-order satellites are close to the first-order satellite (see Fig. 1) and that a constant ratio occurs between the intensities of any group of 1, 5, or 7 satellites. We may understand this qualitatively by realizing that there is an overall structure factor that varies slowly across the Brillouin zone, and because the 1, 5, and 7 satellites are close to each other they all have similar structure factors. The amplitude, of course, decreases rapidly as the order n increases. However, for the third (and ninth) orders the satellites are in a part of reciprocal space far from the first-order satellite (see Fig. 1). For example, the four first-order satellites that surround the scan shown in Fig. 6 have structure factors [$F_c(2^+,0^+,0^+)=0.011$; $F_c(2^+,0^+,1^-)=0.070$; $F_c(3^-1^-1^-)=0.052$; and $F_c(3^-,1^-,0^+)=0.050$]; so that it is not clear what the value of the structure factor will be for the third-order satellites. Accordingly, we have measured a number of third-order satellites and their structure factors are given in Table II. Surprisingly, these show very little intensity variation except for a dependence on the h value.

In Table III we collect together various characteristics of the satellites as deduced from fitting the reflections in Figs. 5 and 6.

The temperature dependencies of the intensities of the

TABLE II. Structure factors of third-order satellites at 15 K. The (hkl) values are where the satellites are observed, with l^- corresponding to $l-3q_z$ and l^+ to $l+3q_z$ positions. The parent first-order positions are indicated so that the satellite should be indexed as $(H,K,L)\pm3\mathbf{q}^i$, where the sign after l indicates whether the satellite is ±3, and the column labeled $\mathbf{q}^i$ gives the q vector using Eq. (2). Reference should be made to Sec. III D for further details of indexing. Units are normalized to the strongest Bragg peak $F(200)=1$, as in Ref. 5. We have chosen an indexing scheme with $q_z>0$.

h	k	l	H	K	L	$\mathbf{q}^i$	H	K	L	$-\mathbf{q}^i$	10^3F_0 (±1)
2.5	3.5	1^-	4	4	1	1	1	3	1	3	17
		0^+	1	3	0	1	4	4	0	3	17
2.5	2.5	2^-	4	2	2	2	1	3	2	4	13
		1^+	1	3	1	2	4	2	1	4	16
2.5	2.5	1^-	4	2	1	2	1	3	1	4	15
		0^+	1	3	0	2	4	2	0	4	12
2.5	1.5	3^-	4	2	3	1	1	1	3	3	20
		2^+	1	1	2	1	4	2	2	3	19
2.5	1.5	2^-	4	2	2	1	1	1	2	3	15
		1^+	1	1	1	1	4	2	1	3	17
2.5	1.5	1^-	4	2	1	1	1	1	1	3	18
		0^+	1	1	0	1	4	2	0	3	18
2.5	0.5	3^-	4	0	3	2	1	1	3	4	13
		2^+	1	1	2	2	4	0	2	4	16
2.5	0.5	2^-	4	0	2	2	1	1	2	4	18
		1^+	1	1	1	2	4	0	1	4	16
2.5	0.5	1^-	4	0	1	2	1	1	1	4	14
		0^+	1	1	0	2	4	0	0	4	17
1.5	1.5	3^-	3	1	3	2	0	2	3	4	8
		2^+	0	2	2	2	3	1	2	4	7
1.5	1.5	2^-	3	1	2	2	0	2	2	4	9
		1^+	0	2	1	2	3	1	1	4	10
1.5	1.5	1^-	3	1	1	2	0	2	1	4	8
		0^+	0	2	0	2	3	1	0	4	8
1.5	0.5	3^-	3	1	3	1	0	0	3	3	12
		2^+	0	0	2	1	3	1	2	3	12
1.5	0.5	2^-	3	1	2	1	0	0	2	3	11
		1^+	0	0	1	1	3	1	1	3	10
1.5	0.5	1^-	3	1	1	1	0	0	1	3	10
		0^+	0	0	0	1	3	1	0	3	11

TABLE III. Characteristics of n-order satellites in α-U at 15 K. The peaks considered are shown in Figs. 5 and 6. ht refers to the peak height, Δ_0 to the observed FWHM, Δ_{int} to the intrinsic FWHM (corrected for instrumental resolution), Δ is the value in Å^{-1} along c^*, ζ is the coherence length $=2\pi/\Delta$. The structure factors are normalized to the first order. The F_c^{sw} values assume a square-wave modulation in which $A(n)=A(1)/n$ (see text). The calculated values F_{c1} and F_{c2} are discussed in the text. The Δ value for $n=1$ has been taken from the x-ray experiment (Ref. 9). In the neutron case it is resolution limited at 0.014 rlu. Uncertainties in parentheses refer to the least-significant digit.

							structure factors $\times 10^3$		
n	ht	Δ_0 (rlu)	Δ_{int} (rlu)	Δ (Å^{-1})	Δ/n (Å^{-1})	ζ (Å)	F_0	F_c^{sw}	F_{c1}	F_{c2}
1	15 800			0.014(1)	0.014(1)	450	[74]	[74]	[74]	[74]
3	600	0.023(2)	0.018(2)	0.023(2)	0.008(1)	~270	17(1)	25	27	24
5	120	0.047(3)	0.044(3)	0.056(3)	0.011(2)	~110	11(1)	15	20	13
7	25	0.060(10)	0.058(10)	0.074(10)	0.011(2)	~85	5(1)	10.6		8
9	~5	0.06(2)	0.06(2)	0.08(2)	0.008(2)	~80	2(1)	8.2		4

third- and fifth-order satellites are shown in Fig. 7. We note that the third-order satellites develop somewhat before the fifth-order satellites as is expected since the third-order satellites represent the first component of the squaring process, and that both harmonics show considerable hystersis.

E. Measurement of the q_z component

The value of the q_z component found in the early work[5] was 0.182 rlu. This was determined by measuring the distance of the strong first-order satellites from the average structure reciprocal-lattice points. The discovery of higher-order satellites allows a greater precision in the measurement of q_z because the peaks are a distance nq_z away from a lattice point, where n is the satellite order. The results of using the $n=3$ and 5 satellites are shown in Fig. 8. In principle, the $n=7$ satellites give even greater precision, but their widths (see Table III) are very large and their intensity is low (Fig. 5), so it is not practical to use these satellites.

We find that q_z remains constant below 20 K and the neutron work gives a value of $q_z=0.1858(6)$ rlu. As we shall see, this is significantly different from the value (0.1818) obtained by x-ray experiments.[9] The previously reported value[2,3] of 0.1820(20) was determined using the first-order satellites. By using the higher-order satellites we can clearly increase the precision in q_z and place confidence on differences of 0.0030 rlu.

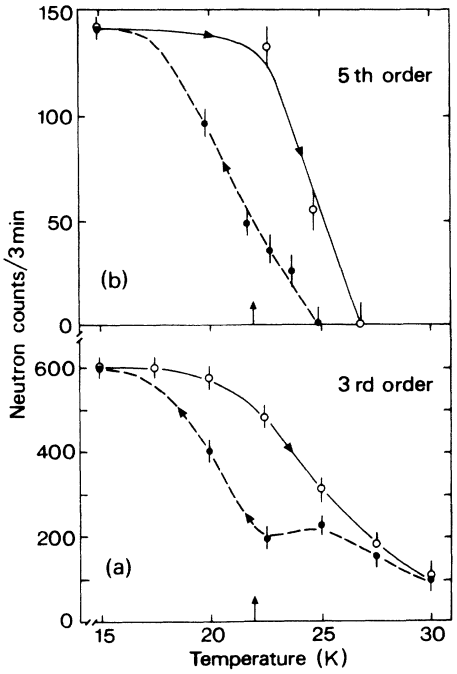

FIG. 7. Temperature dependence of (a) third-order satellite at the position $(2.5,0.5,3q_z)$ and (b) fifth-order at position $(2.5,\frac{1}{6},2-5q_z)$. Solid (open) points correspond to cooling (heating). The arrow marks 22 K.

IV. DISCUSSION

A. Average structure

For $q_x=\frac{1}{2}$ van Smaalen and George[7] have listed all the possible superspace groups in Table II of their paper.

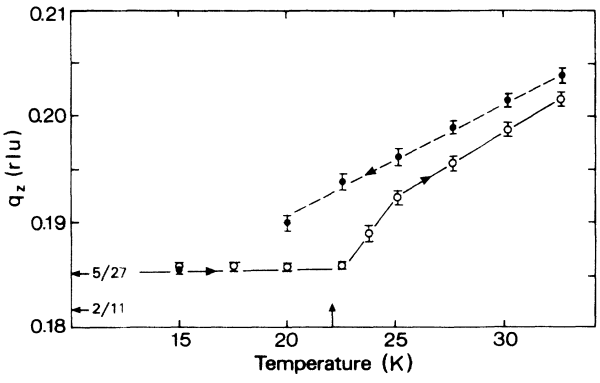

FIG. 8. Variation of q_z (in reciprocal-lattice units) with temperature as measured from both the third- and fifth-order satellites. Solid (open) points correspond to cooling (heating). The arrow marks 22 K. The solid line at low temperature is the value 5/27.

There are 16 in total, five with orthorhombic symmetry, nine with monoclinic, and two triclinic. Eight of the groups preserve the high-temperature *C*-face centering. Our observations may be related first to whether the modulated phase shows *C*-face centering. We have discussed how vectors $(\mathbf{q}^{(1)},\mathbf{q}^{(4)})$ are coupled to give satellites either in addition or subtraction (Fig. 3 illustrates such a satellite). In the situation ($T<37$ K) that $q_x=\frac{1}{2}$ the combination of $\mathbf{q}^{(1)}$ and $\mathbf{q}^{(4)}$ implies a reciprocal-lattice vector displacement of (1,0,0). This is not a permitted translational if *C*-face centering is present. Our measurements show directly that the *C*-face centering does *not* exist in the modulated phase below 37 K. Group Nos. 9–16 in the superspace group table are therefore excluded.

A further reduction in the possible superspace groups may be obtained by noting that groups no. 1–5 with orthorhombic symmetry require the presence of the vectors $\mathbf{q}^{(1)}\pm\mathbf{q}^{(2)}$ and $\mathbf{q}^{(1)}\pm\mathbf{q}^{(3)}$. We have searched extensively for these types of satellites but found no evidence for their existence. This excludes groups 1–5 within the orthorhombic symmetry.

We are left with three space groups having monoclinic symmetry: No. 6, P2/m11; No. 7, P211; and No. 8, Pm11. Walker[8] has shown that No. 8 does not allow a first-order lock-in transition along q_x (to the value of $\frac{1}{2}$ at 37 K). Since this transition is observed,[9] No. 8 is excluded. The difference between No. 6 and No. 7 is that No. 6 has an inversion center, whereas this is absent in No. 7. We cannot distinguish between these two in our measurements by systematic absences or symmetry considerations. We note, however, that van Smaalen and George have obtained a lower *R* factor for No. 7 (7.1% as compared to 10.6% for No. 6). This favors No. 7, P211, as the superspace group in the CDW phase below 37 K.

B. Lock-in of the q_y component and higher harmonics

The development of higher harmonics in the CDW modulation is clearly associated with the lock-in transition of q_y. The third-order harmonic is visible above 30 K, but only has appreciable intensity below ~22 K. The fifth-order harmonic grows very rapidly around this temperature. We have not tried to measure the seventh- and ninth-order harmonics as a function of temperature. There is strong hysteresis in both the third- and fifth-order harmonics, which we ascribe to domain motion near the 22-K transition. Very unusual effects were also observed at this temperature in the electron microscopy study.[6] Hysteresis effects are also evident in the q_z parameter (Fig. 8). Indeed, it would appear that a range of q_z values could be obtained if different thermal cycling procedures were used. The theory of Grubel *et al.*[9] suggests that q_z should also lock in to the commensurate value of 1/6, but that it is prevented from doing so by other subtle energetic considerations. The x-ray experiments[9] find clear evidence for a value $q_z=0.1818$, i.e., close to $\frac{2}{11}$, whereas the neutron value is significantly higher than this. However, the neutron value of 0.1858(6) is close to $\frac{5}{27}=0.1852$. This latter is a possible commensurate value suggested by the analysis of Ref. 9. We thus have the unusual situation that the surface values, as seen by x-rays, and bulk values, as seen by neutrons, of the CDW wave vector are slightly different with respect to the q_z component. Note that this difference is only 1.8% of c^*, and a much smaller percentage of the total **q** vector, but it no doubt represents the results of stress effects, which will predominantly influence the surface. We have seen from Fig. 8 how sensitive q_z is to thermal cycling, so that the domain structure along the **c** direction is clearly complicated.

There is another interesting aspect of the third-order satellites in that when $q_y=\frac{1}{6}$ the satellites at $1-3q_y$ and $0+3q_y$ are at the same place. Thus returning to Fig. 1 the satellites at $(2.5,0.5,1-3q_z)$ may be indexed either as $(1,1,1)+3\mathbf{q}^{(4)}$ or as $(4,0,1)-3\mathbf{q}^{(2)}$, where $\mathbf{q}^{(i)}$ is defined in Eq. (2). Since the domain states of the system are $\{\mathbf{q}^{(1)},\mathbf{q}^{(4)}\}$ or $\{\mathbf{q}^{(2)},\mathbf{q}^{(3)}\}$, according to van Smaalen and George[7] and Walker,[8] these satellites should arise from different physical regions of the crystal. This means there should be *no* coherence between them and the intensities, rather than amplitudes, should be added. On warming, q_y breaks away from the value of $\frac{1}{6}$ (Fig. 4) so that $1-3q_y\neq 0+3q_y$ and *two* satellites appear instead of one. However, in our present experiment the q_y resolution is rather poor, especially as we have used a vertically focusing monochromator, so that it is only at ~27 K that the two satellites can be resolved. By this temperature they have already fallen to a small intensity [Fig. 7(a)]. By monitoring their intensity as a function of temperature it is clear that the intensities rather than amplitudes are added when $q_y=\frac{1}{6}$.

C. Squaring of the CDW modulation

The discovery of higher-order satellites in α-U below about 30 K (see Fig. 7) implies a change in the wave form of the distortion. Earlier work[5] showed that the second-order satellites were of the approximate order of magnitude of that expected from a pure sinusoidal distortion. As is well known, the appearance of odd-order satellites only (1, 3, 5, 7, and 9, etc.) signifies the squaring of the modulation. Thus the Fourier components can be arranged such that the displacement of *all* atoms are either $\pm\epsilon$.

The Fourier expansion of a square-wave modulation of magnitude ϵ is

$$\epsilon=\frac{\pi}{4}A\sum_{m=1,\text{odd}}^{\infty}\frac{1}{m}\sin(2\pi m\,\mathbf{q}\cdot\mathbf{r}^0)\ , \tag{3}$$

where A is the amplitude of the first-order harmonic, $\mathbf{r}^0$ gives the atom position, and the sum is over $m=$odd orders only. The structure factor for the n-order satellite is given by

$$F_c^n\approx J_n(\epsilon\mathbf{a}\cdot\mathbf{Q})$$
$$\approx(\epsilon\mathbf{a}\cdot\mathbf{Q})^n\ , \tag{4}$$

where J_n is the Bessel function of order n and the expansion is valid when $(\epsilon\mathbf{a}\cdot\mathbf{Q})$ is small. The intensities are then proportional to Q^2. An approximate relationship

between the different harmonics, when ϵ is small and terms in ϵ^2 are negligible, is that the amplitude $A(n)$ of order n is $A(n) \simeq A(1)/n$. (This result is exact for a magnetic modulation where the modulation concerns the magnitude of the moment rather than a displacement.) This relationship, normalizing to the first order structure factor being 0.074, is given in the F_c^{sw} column of Table III. A more-precise calculation assuming a square-wave modulation of 6^+, 6^- displacements is given under the column heading F_{c1}. Notice that in this (simple) commensurate model ($q = \frac{1}{6}$), orders above 5 overlap with lower orders and are thus already included. The particular model of displacements along the c axis with atoms separated by $c/2$ gives zero intensity at l=odd positions.

The experimental values of F_0 clearly fall more rapidly with increasing n than either of the above models (i.e., as compared to F_c^{sw} or F_{c1} in Table III). This means that the squaring of the wave is by no means complete. Furthermore, the higher-order satellites are considerably broader in the $\mathbf{c}^*$ direction than the experimental resolution function. This may be best seen in Fig. 5, where the fifth- and seventh-order satellites are clearly wider than the first. These widths are given in Table III and then deconvoluted with the instrumental resolution to give an intrinsic full width at half maximum Δ_{int} in reciprocal-lattice units (and Δ in Å^{-1}) along $\mathbf{c}^*$. Using the relationship that $\zeta = 2\pi/\Delta$, we may deduce the correlation length ζ along $\mathbf{c}$ and this is found to vary from ~ 500 to ~ 80 Å. A point of interest, although we do not completely understand its significance, is that Δ/n is a constant within experimental uncertainty. Qualitatively, what this signifies is that the higher harmonics have a progressively smaller coherence length, which varies (approximately) with the order n.

What about the correlation lengths in the $\mathbf{a}^*$ and $\mathbf{b}^*$ directions? We have not examined these in detail but we find that the peaks are sharper in these two directions, indicating that the correlations are at least 400–500 Å. Particularly in the $\mathbf{a}^*$ direction, in which the unit cell is simply twice the primitive cell, we find the peaks are almost resolution limited, and even in the higher resolution synchrotron x-ray experiment[9] only a small broadening could be observed. We should note that both q_x and q_y have simple commensurate values so that the longer-range correlations in these directions are to be expected.

The squaring of the modulation is most abrupt around 22 K, the temperature at which q_y locks to the value of $\frac{1}{6}$ (Fig. 4), but a tendency to form a square wave is already in evidence at 30 K as judged by the temperature dependence of the third-order harmonic (Fig. 7). Very considerable, and complicated, hysteresis effects are observed in the region of 20 to 27 K. These can be associated with the complex domain motion, which has been seen in this temperature region with the electron microscope.[6]

We have also made an attempt to refine the amplitude of the third-order harmonic using the data of Table II. Since the intensities are the sum of two satellites arising from very different (see *HKL* indices in Table II) fundamental reflections, there is no method to simply deconvolute these intensities. Using a model with displacements along the $\mathbf{a}$ axis only, we can quite easily reproduce the intensities to an R factor of $\sim 14\%$ with a third-order harmonic displacement wave of amplitude 25% of the first-order harmonic. This is what one might anticipate from Table III, where the perfect square wave would have an amplitude ratio of about 1:3 with respect to the first-order harmonic, but the ratio of the F_0 values is $17/74 = 0.23$. Diffraction experiments cannot give information on the phase relationship between these two displacement waves, but it makes physical sense to assume they are such as to produce a partial squaring of the displacement wave.

D. Physical models for the displacement

The $\mathbf{q}$ vector at low temperature is

$$\mathbf{q} = \tfrac{1}{2}\mathbf{a}^* + \tfrac{1}{6}\mathbf{b}^* + \tfrac{5}{27}\mathbf{c}^* ,$$

where $\mathbf{a} = 2\pi/a$, etc., and $a = 2.844$ Å, $b = 5.5689$ Å, and $c = 4.9316$ Å. If we approximate $5/27 \simeq 1/6$, then the total repeat unit cell in the CDW state at low temperature is $2\mathbf{a} \times 6\mathbf{b} \times 6\mathbf{c}$, a total of 288 atoms of uranium with a volume of 5926 Å.[3] The square-wave modulation is, of course, a simple one where all the atoms are displaced $\pm\epsilon$ from their equilibrium position, and is made up of odd-order Fourier components. If the amplitude of the first component is $A(1)$, then the square-wave displacement will be $\epsilon = (\pi/4)A(1)$.

However, this model does not describe accurately the situation in α-U because $q_z \neq \frac{1}{6}$ and the harmonics are *not* in the correct ratio of A/n, as shown in Table III. Reference 9 has shown that there is a potential for driving both q_y and q_z to the commensurate value of $\frac{1}{6}$ but this is not achieved with q_z. Instead, $q_z = 5/27$, which in the "phase-slip" model[9] implies a precise ordering of the displacements. Can we determine whether this is a likely modulation?

In the commensurate case $q_z = \frac{1}{6}$ and the displacement on sequential atoms may be written $6^+, 6^-$. The structure factors of the different satellites (1,3,5) are given in the column F_{c1}. The phase-slip model[9] corresponds to introducing a fault every p planes. The simplest fault is one after every 11 atoms, the precise arrangement will then be $6^+, 5^-, 5^+, 6^-$, and the $q = 2/11$ or two repeat units after 11 cells (i.e. 22 atoms). As shown in Refs. 9 and 13, the $q = 5/27$ state is made up of a fault every nine atomic layers. The sequence of displacements is

$$6^+, 5^-, 5^+, 6^-, 5^+, 5^-, 6^+, 5^-, 5^+, 6^-$$

with 5 repeats in 27 unit cells (54 atoms). We have performed a calculation using a simple, one-dimensional model and the results are given in the column F_{c2}.

The agreement between F_{c2} and F_0 is clearly acceptable, except perhaps for $n = 3$, and suggests that this complex pattern of displacement may occur along the $\mathbf{c}$ axis in the CDW state. However, we should also recall that the coherence length of the Fourier components of different order is progressively shorter as n increases. This will result in a decrease in the long-range order and

a loss in intensity of the higher orders. Modeling such an effect is outside the scope of this article. The displacement wave along **c** is not a pure square wave (whereas it can be in the **a** and **b** directions because of the commensurate q components) and the complex displacement pattern suggested by the phase-slip model[9,13] gives reasonable agreement with experiment.

V. SUMMARY

The important results of our neutron experiments may be summarized as follows.

(i) The 2**q** state predicted by Walker[8] and van Smaalen and George[7] has been verified experimentally. The C-face-centering symmetry operation does not exist in the CDW state of α-U below 37 K. The superspace group of the CDW state is either P2/m11 or P211, where structure refinements favor the latter.[7] Monodomain samples, or at least an unequal domain population, need to be produced before further progress is to be made.

(ii) At 37 K the q_x component locks in to the commensurate value of $\frac{1}{2}$, although this is observed better with the high resolution available with synchrotron x rays.[9] The q_y component locks in to a commensurate value of $\frac{1}{6}$ at 22 K (Fig. 4). This is the explanation of the 22-K transition first seen in thermal-expansion measurements.[12]

(iii) The q_z component has an unusual behavior (Fig. 8). The neutron results suggest that q_z attains a value 5/27 at low temperature, which is different from the x-ray value[9] of 2/11. We ascribe this difference to strain effects that may vary essentially between the surface (x rays) and bulk of the material (neutrons). Both these unusual values may be understood in the "phase-slip" model.[9]

(iv) Perhaps the most important result of our experiments has been the observation of higher-order harmonics (up to ninth order) in the low-temperature form. We have observed coherent diffraction intensities down to a level of 10^{-6} of the principal Bragg peaks. The observation of odd-order satellites only implies that a squaring of the distortion modulation of the CDW occurs between 30 and 20 K. However, complete squaring is not observed, even at low temperatures (Table III). Furthermore, the correlation lengths of the higher-order harmonics decrease, approximately with the relationship $1/n$, where n is the harmonic order.

(v) The reader will no doubt be surprised to be presented with a different model in this paper for the atomic displacements at low temperature compared with that to be published in Ref. 9. In this latter reference, the phase-slip model is used to explain the particular values of q_z found with both x rays and neutrons, and can quantitatively account for the magnitude of the fifth- and seventh-order satellites (Fig. 5). However, the model does not predict a third-order satellite. This is not surprising as it involves only one sinusoidal modulation, the first Fourier harmonic. Conversely, the models discussed in the present paper *start* from an assumption of a complete square wave. This is shown to be also quantitatively incorrect, especially when the higher orders are considered. Nor can it give an explanation of the particular values of q_z. The *true* picture of the displacements in the CDW state undoubtedly lies between these extreme models, and can probably be obtained by starting from either model and adding additional terms.

With the exception of the "Smith" satellites,[1] the diffraction effects are now reasonably well understood in the CDW state in α-U. To gain a complete understanding of *why* α-U distorts in this way is much more complex. We postulate that the CDW arrangement is a compromise between the elastic energy (in terms of requiring the atoms to remain at their equilibrium positions) and the electronic energy derived from the strong hybridization of the $5f$ and $6d$ electrons. It is known that the $5f$ orbitals are extremely anisotropic in real space and that they form part of the bonding states[14] in α-U. In general terms the electronic energy is lowered by gaps in the Fermi surface that are opened by the CDW distortion. To understand this in detail will require extremely precise band-structure calculations with the correct α-U structure and then consideration of the electron-phonon interaction. The phonon instability, which arises undoubtedly from electronic effects, is certainly the driving force for the CDW distortion. de Haas–van Alphen experiments would also be of great interest.

Finally, we should point out that although α-U is at present the only element exhibiting a spontaneous CDW, we believe that similar effects will be found in Np and Pu. In both of these materials the $5f$ electrons participate strongly in the bonding,[14] and in both elements a series of unusual, and still not explained, anomalies have been found in physical property measurements.[15] Unfortunately, to make further progress along this line we require single-crystal samples, which, because of the complicated phase diagrams and radioactivity, are very difficult to produce.

ACKNOWLEDGMENTS

We thank Alain Delapalme for his participation and enthusiasm early in this project. Using the D-10 high-resolution diffractometer was made easier by the excellent technical help of René Chagnon. One of the authors (J. C. Marmeggi) wishes to thank Jacques Villain for valuable discussions. The research of S. van Smaalen is supported by the Royal Dutch Academy of Arts and Sciences (KNAW). G.H.L. thanks Gerhard Grubel, John Axe, and Doon Gibbs of Brookhaven National Laboratory for discussions on this project.

[1]H. G. Smith, N. Wakabayashi, W. P. Crummett, R. M. Nicklow, G. H. Lander, and E. S. Fisher, Phys. Rev. Lett. **44**, 1612 (1980).

[2]J. C. Marmeggi and A. Delapalme, Physica B+C **120B**, 309 (1980).

[3]J. C. Marmeggi, A. Delapalme, G. H. Lander, C. Vettier, and N. Lehner, Solid State Commun. **43**, 577 (1982).

[4]W. P. Crummett, H. G. Smith, R. M. Nicklow, and N. Wakabayashi, Phys. Rev. B **19**, 6028 (1979).

[5]H. G. Smith and G. H. Lander, Phys. Rev. B **30**, 5407 (1984).

[6]C. H. Chen and G. H. Lander, Phys. Rev. Lett. **57**, 110 (1986).

[7]S. van Smaalen and T. F. George, Phys. Rev. B **35**, 7939 (1987); S. van Smaalen and C. Haas, Solid State Commun. **55**, 1027 (1985).

[8]M. B. Walker, Phys. Rev. B **34**, 6830 (1986).

[9]G. Grubel, J. D. Axe, D. Gibbs, G. H. Lander, H. G. Smith, J. C. Marmeggi, and T. Brückel (unpublished).

[10]S. Pujol, R. Chagnon, and C. M. E. Zeyen (unpublished).

[11]C. S. Barrett, M. H. Mueller, and R. L. Hitterman, Phys. Rev. **129**, 625 (1963).

[12]M. O. Steinitz, C. E. Burleson, and J. A. Marcus, J. Appl Phys. **41**, 5057 (1970).

[13]J. Bohr *et al.*, Physica B+C **B159**, 93 (1989); Physica A **140**, 349 (1986).

[14]See, for example, M. S. S. Brooks, B. Johansson, and H. L. Skriver, in *Handbook on the Physics and Chemistry of the Actinides,* edited by A. J. Freeman and G. H. Lander (North-Holland, Amsterdam, 1984), Vol. 1, pp. 153ff.

[15]J. M. Fournier and R. Troc, in Ref. 14, Vol. 2, pp. 29ff.

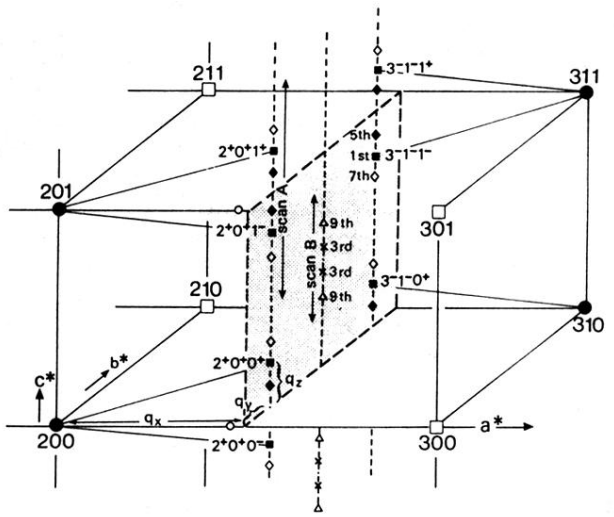

FIG. 1. Schematic of reciprocal space in α-U. Since the high-temperature structure is C face centered, allowed lattice points (solid circles) have $h+k=$even. The non-C-face-centered points are shown as open squares. Satellites are ■ (first), × (third), ♦ (fifth), ◇ (seventh), and △ (ninth). The position of two of the satellites from the secondary modulation—the so-called "Smith" satellites (Ref. 1)—are shown as open circles.